A New Nomenclature for Cry1Ab Proteins Reflecting 3-D Structure Differences

Liu Xiaoping[1] and Lin Yi[1*]

[1]*Department of Bioengineering and Biotechnology, College of Chemical Engineering, Huaqiao University, 361021, Xiamen, Fujian, China.*

Authors' contributions

This work was carried out in collaboration between both authors. Author LX performed the statistical analysis, wrote the protocol, wrote the first draft of the manuscript and managed literature searches. Author LY designed the study, managed the analyses of the study and literature searches. Both authors read and approved the final manuscript.

Original Research Article

ABSTRACT

Cry1Ab proteins produced by the insecticidal bacterium *Bacillus thuringiensis* are mostly studied and applied, facing the challenge of insect resistance. The 3-D structure of the toxic core for all available 34 Cry1Ab proteins were constructed by the method of homology modeling. Based on the secondary structure pattern, four different groups were identified and named as Cry1AbⅠ, Cry1AbⅡ, Cry1AbⅢ, and Cry1AbⅣ. The three Cry1Ab proteins, Cry1Ab2, Cry1Ab7 and Cry1Ab28 were recognized as Cry1AbⅡ, Cry1AbⅢ, and Cry1AbⅣ, respectively. The other 31 Cry1Ab proteins were grouped as Cry1AbⅠ, and were further divided into three subgroups based on 3-D structural differences, Cry1AbⅠ3 (Cry1Ab33 only), Cry1AbⅠ2 (Cry1Ab31 only), and Cry1AbⅠ1 (the rest of Cry1AbⅠ). The structural differences among different Cry1Ab groups and subgroups were presented in details. The insecticidal activities of different Cry1Ab groups and subgroups were also discussed. It was worthy to speculate that the only difference in 3-D structure, residues 447-449 form β-sheet in Cry1AbⅠ vs loop in Cry1AbⅢ, resulted in Cry1AbⅠ inactive vs Cry1AbⅢ

_____

Corresponding author: E-mail: lyhxm@hqu.edu.cn;

active against mosquito. The data obtained from the present in *silico* study provided new insights into structure-function relationship of Cry1Ab proteins.

Keywords: Bacillus thuringiensis; Cry1Ab; structure-based nomenclature; structure-function relationship; mosquito-specific motif.

1. INTRODUCTION

Bacillus thuringiensis, commonly known as Bt, is a Gram positive bacterium that occurs naturally in the soil around the world. For decades, bacteriologists have known that some strains of Bt kill certain insects and that the toxic substance responsible for the insects death is a protein generally referred to as parasporal crystal proteins (Cry proteins) [1]. These Cry proteins produced by Bt is widely used in biopesticide formulations and transgenic crops for insect control. The mode of action of Cry toxins is still a matter of investigation, generally, following ingestion by insects, they are activated by gut proteases and by binding to specific receptors on midgut epithelial cells [2]. Receptor binding induces the conformational change in the toxin necessary for membrane insertion, where it forms ion selective channels via oligomerization of toxin monomers, leading to cell lysis and finally to larval death [3,4].

The existing nomenclature ranks demarcate the four levels, and the boundaries represent approximately 95, 78, and 45% sequence identity. To date, the Cry genes have been classified as Cry1 to Cry73, Cyt1, Cyt2 and Cyt3 are ranked according to their homology [5]. So far only eight structures of Cry toxins from Bt namely Cry1Aa (PDB ID: 1CIY) [6], Cry2Aa (PDB ID: 1I5P) [7], Cry3Aa (PDB ID: 1DLC) [8], Cry3Bb (PDB ID: 1JI6) [9], Cry4Aa (PDB ID: 2C9K) [10], Cry4Ba (PDB ID: 1W99) [11], Cry8Ea (PDB ID: 3EB7) [12] and Cry5Ba (PDB ID: 4D8M) [13] have been determined by X-ray crystallographic methods. However, Cry11Bb [14], Cry5Aa [15], Cry5Ba [16], Cry3A [1], Cry1Id [17], Cry30Ca2 [18], Cry10Aa [19], and Cry1Ib9 [1] have been predicted by homology modeling methods. Furthermore, Kashyap et al. [20-24] predicted the structure of Cry1Ab15, Cry1Ab16, Cry1Ab17, Cry1Ab19 and Cry1Ab21 by homology modeling. These reports have supported the three domains hypothesis for the toxic core of Cry proteins revealing domain Ⅰ to be consisting of α-helical bundle, domain Ⅱ of antiparallel β sheets and domain Ⅲ made up of β sandwich [6].

Although Cry1Ab have been mostly studied and used, few efforts have been focused on the structural relationships among Cry1Ab members. To establish a new nomenclature which provide structural relationships among Cry proteins helping us to learn more about the relationship between structural differences and activities, the secondary structure and 3-D structure of all available 34 Cry1Ab proteins were constructed by the method of homology modeling, then different groups and subgroups were identified based on the secondary structure pattern and 3-D structure comparison.

2. MATERIALS AND METHODS

The reviewed full length amino acid sequences of all available Cry1Ab proteins were obtained from the National Center for Biotechnology Information (NCBI) database (http://www.ncbi.nlm.nih.gov/GenBank). The sequence accession numbers were AAA22330, AAA22613, AAA22561, BAA00071, CAA28405, AAA22420, CAA31620, AAA22551, CAA38701, A29125, I12419, AAC64003, AAN76494, AAG16877, AAO13302, AAK55546, AAT46415, AAQ88259, AAW31761, ABB72460, ABS18384, ABW87320, HQ439777, HQ439778, HQ685122, HQ847729, JN135249, JN135250, JN135251, JN135252, JN135253, JN135254, AAS93798, KC156668, respectively.

The 3-D structure of target proteins was predicted by using the server SWISS-MODEL (http://swissmodel.expasy.org/) [25] which is a fully automated protein structure homology-modelling server. The Ramachandran plot assessments were conducted by submitting the PDB files to RAMPAGE server (http://mordred.bioc.cam.ac.uk/). Alignment of those structures that showed secondary structure and 3-D structure similarities and differences were directly performed in Pymol software, and sequence alignment among the four groups of Cry1Ab was generated using ClustalX program. Insecticidal activity data was obtained from the web of Toxin Nomenclature (http://www.glfc.forestry.ca/bacillus/).

3. RESULTS

3.1 3-D Structures of the Toxic Core of Available 34 Cry1Ab Proteins were Constructed by Homology Modeling

The structural models of the Cry1Ab toxic core were obtained comprising of 578 amino acids out of 1155 long primary structure, approximately. Sequence alignment showed an average of 88.5% identity between each Cry1Ab and Cry1Aa (PDB: 1CIY). All the 3-D structures of the toxic core of 34 available Cry1Ab proteins were constructed by homology modeling and evaluated by Ramachandran plot. Comparison of structures among the members of Cry toxin family revealed that Cry1Ab shares similar architecture with them and forming a wedge shape. The predicted structure of toxic core is comprised of three putative domains (Fig. 1). A Ramachandran plot indicated that most (95 %) residues have φ and ψ angles in the core and allowed regions (Fig. 2).

In the absence of an experimentally determined structure, comparative or homology modeling can sometimes provide a useful 3-D model for a protein that is related to at least one known protein structure [26]. It is observed that a model tends to be reliable if identity percentage between the template and target protein is above 40%. Low degree of reliability arises when identity decreases below 20% [27]. All 34 Cry1Ab proteins shared more than 85 % identity between them and template protein (Cry1Aa), and the results of Ranachandran plot all surpass 95%, hence, the models constructed in this study are reliable.

3.2 The 34 Cry1Ab Proteins are Divided into Four Groups Based on the Secondary Structure Patterns of Toxic Core

The secondary structure pattern of the toxic core of the 34 Cry1Ab proteins was characterized based on the structural models (Table 1). Four different groups were identified and named as Cry1AbⅠ, Cry1AbⅡ, Cry1AbⅢ, and Cry1AbⅣ (Table 2). The Cry1AbⅠ group included 31 Cry1Ab proteins, Cry1Ab1, Cry1Ab3, Cry1Ab4, Cry1Ab5, Cry1Ab6, Cry1Ab8, Cry1Ab9, Cry1Ab10, Cry1Ab11, Cry1Ab12, Cry1Ab13, Cry1Ab14, Cry1Ab15, Cry1Ab16, Cry1Ab17, Cry1Ab18, Cry1Ab19, Cry1Ab20, Cry1Ab21, Cry1Ab22, Cry1Ab23, Cry1Ab24, Cry1Ab25, Cry1Ab26, Cry1Ab27, Cry1Ab29, Cry1Ab30, Cry1Ab31, Cry1Ab32, Cry1Ab33 and Cry1Ab34. The other three Cry1Ab proteins, Cry1Ab2, Cry1Ab7, and Cry1Ab28, however, were recognized as CryAbⅡ, CryAbⅢ, and CryAbⅣ, respectively.

Cry1AbⅠ, Cry1AbⅡ and Cry1AbⅢ domainⅠ was composed of N-terminal 235 amino acid residues folded into a bundle of 8 amphipathic α-helices and 1 small β-strand. Cry1AbⅣ domainⅠ, however, was composed of N-terminal 234 amino acid residues. As with other Cry toxins, DomainⅡ of Cry1Ab consists of three Greek key β sheets arranged in β prism topology. It was composed of 205 amino acid residues, with 4 α-helices and 11 β strands in Cry1Ab Ⅰ and Cry1Ab Ⅳ, and 10 β strands in Cry1Ab Ⅲ. DomainⅡ of Cry1AbⅡ, however, consisted of 211 amino acid residues, with 5 α-helices and 8 β strands. Domain Ⅲ comprised residues 480-606 in Cry1Ab Ⅰ and Cry1Ab Ⅲ, 479-605 in Cry1Ab Ⅳ, and 489-607 in Cry1Ab Ⅱ. The amino acid residues of all Cry1Ab Domain Ⅲ are highly conserved.

3.3 The 31 Members of Cry1AbⅠ Group are Further Divided into Three Subgroups Based on 3-D Structural Comparison

The 3-D structural comparison among the 31 members of Cry1AbⅠ indicated that 3-D structure of Cry1Ab31, Cry1Ab33 are different from the rest of Cry1AbⅠ (Fig. 3 and Fig. 4). Thus, Cry1AbⅠ can be further divided into three subgroups, Cry1AbⅠ3 (Cry1Ab33 only), Cry1AbⅠ2 (Cry1Ab31 only), and Cry1AbⅠ1 (the rest of Cry1AbⅠ, Cry1Ab1 as the model) (Table 2). The differences among the Cry1AbⅠ group were found in loops of domainⅡ. The loop β8-β9 in domainⅡ of Cry1AbⅠ1 differ from that of Cry1AbⅠ2 resulted from residue 440 is Phe in Cry1AbⅠ1 vs Leu in Cry1AbⅠ2. The loop β4-β5 is different resulted from residue 369 is Arg in Cry1AbⅠ1 instead of Ser in Cry1AbⅠ3. Both of loops β4-β5 and β8-β9 are different between Cry1AbⅠ2 and Cry1AbⅠ3, which resulted from residue differences Arg369Ser and Leu440Phe.
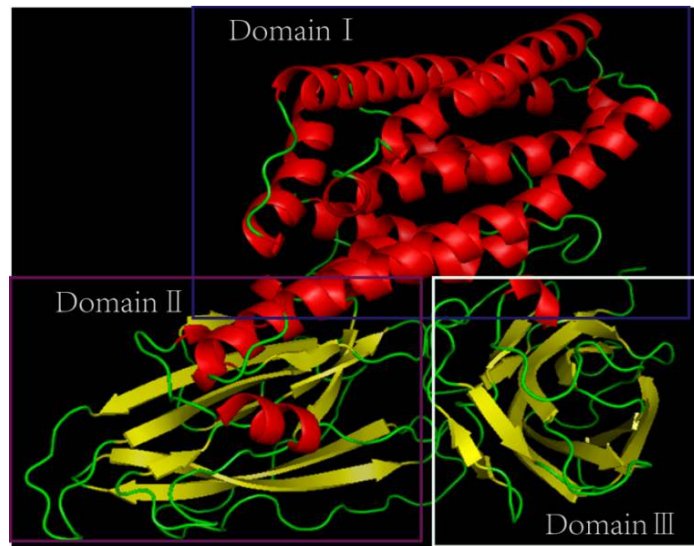
Fig. 1. Cartoon representation of the structure of Cry1Ab toxins
The colored boxes donotes the positions of the different domains
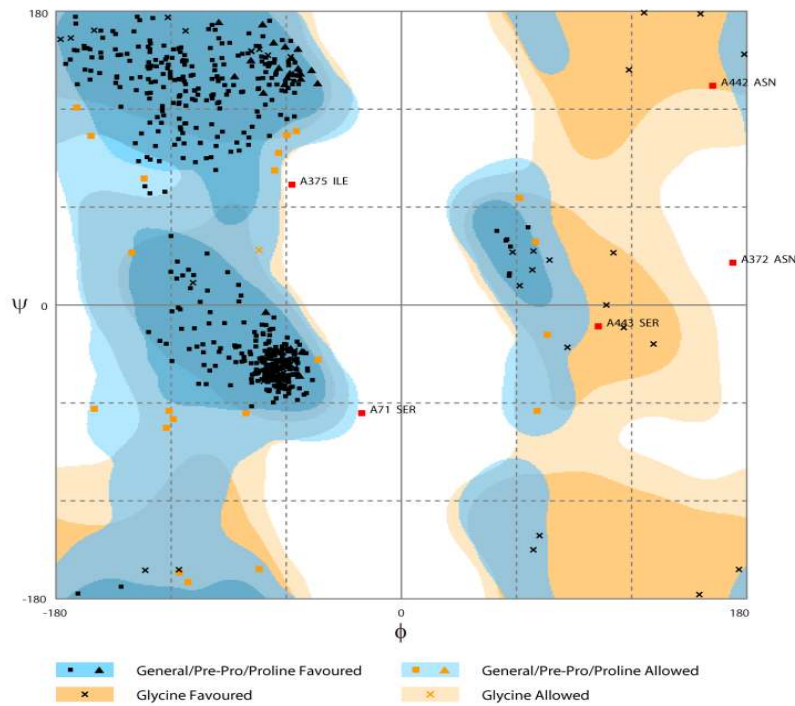
Number of residues in favoured region (~98.0% expected)   : 549 (95.3%)
Number of residues in allowed region (~2.0% expected)   : 22 (3.8%)
Number of residues in outlier region   : 5 (0.9%)

Fig. 2. Evaluation of Cry1Ab1 model. Ramandren plot analysis showing placement of its residues in deduced model
General plot statistics are:549 (95.3 %) residues in favored regions; 22 (3.8 %) of residues were in allowed regions;the outlier residues totals to 5 (0.9 %) only. the plot was generated using RAMPAGE web server (http://mordred.bioc.cam.ac.uk/)

4

a
```
/1ab1h     421   426   431     436   441   446   451   456   461   466   471
LDEIPPQNNNVPPRQGFSHRLSHVSMFRSGFSNSSVSIIRAPMFSWIHRSAEFNNIIPSSQITQIP
/1ab31h    421   426   431     436   441   446   451   456   461   466   471
LDEIPPQNNNVPPRQGFSHRLSHVSMFRSGLSNSSVSIIRAPMFSWIHRSAEFNNIIPSSQITQIP
```
b
```
/1ab1h         361   366   371   376   381   386   391   396   401   406   411
RIVAQLGQGVYRTLSSTLYRRPFNIGINNQQLSVLDGTEFAYGTSSNLPSAVYRKSGTVDSLDEI
/1ab33h    351   356   361   366   371   376   381   386   391   396   401   40
RIVAQLGQGVYRTLSSTFYRSPFNIGINNQQLSVLDGTEFAYGTSSNLPSAVYRKSGTVDSLDEI
```
c
```
/1ab31h        361   366   371   376   381   386   391   396   401   406
RIVAQLGQGVYRTLSSTLYRRPFNIGINNQQLSVLDGTEFAYGTSSNLPSAVYRKSGTVD
/1ab33h    351   356   361   366   371   376   381   386   391   396   4
RIVAQLGQGVYRTLSSTFYRSPFNIGINNQQLSVLDGTEFAYGTSSNLPSAVYRKSGTVD
/1ab31h         416   421   426   431     436   441   446   451   456   461
SGTVDSLDEIPPQNNNVPPRQGFSHRLSHVSMFRSGLSNSSVSIIRAPMFSWIHRSAEFN
/1ab33h    406   411   416   421   426   431   436     441   446   451   4
SGTVDSLDEIPPQNNNVPPRQGFSHRLSHVSMFRSGFSNSSVSIIRAPMFSWIHRSAEFN
```
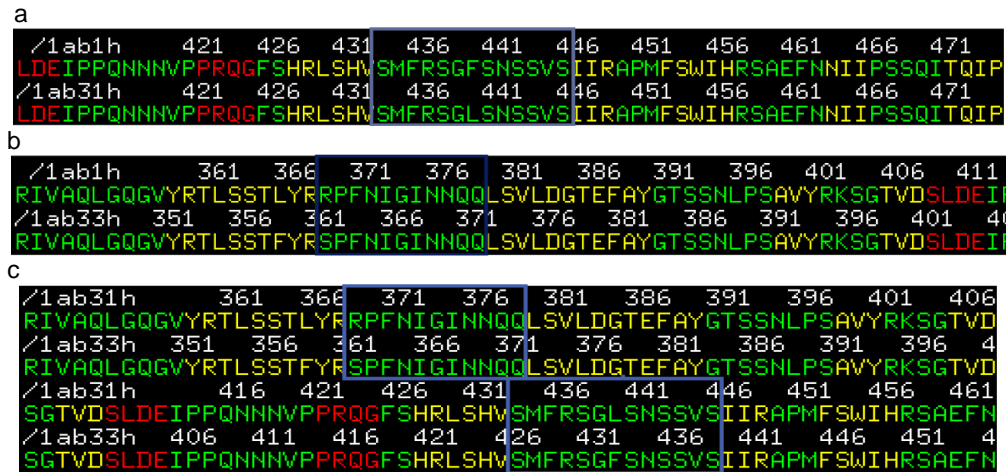
Fig. 3. The partial amino acid sequence alignment of the groups of Cry1Ab Ⅰ
The residues highlighted in red color represent helix; those in yellow represent stand and turn and those in green represent coli and are generated using Pymol software. a The partial amino acid sequence alignment of the Cry1Ab1 with the Cry1Ab31. b The partial amino acid sequence alignment of the Cry1Ab1 with the Cry1Ab33. c The partial amino acid sequence alignment of the Cry1Ab31 with the Cry1Ab33

Cry1Ab Ⅰ 1 showed activities against Lepidoptera, include Noctuidae, Lymantridae, Sphingidae, Pyralidae, Pieridae, Plutellidae, Tortricidae, Chrysopidae and Lasiocampidae (Table 3). Although the insecticidal activity data of Cry1Ab Ⅰ 2 and Cry1Ab Ⅰ 3 were not available, we speculated they had different insecticidal activites compared to Cry1Ab Ⅰ 1 because they differ in the receptor-binding loops in domain Ⅱ.

3.4 Structural Differences between Cry1Ab Ⅰ and Cry1AbⅢ

The toxic core of Cry1Ab Ⅰ was comprised of 13 α-helices, 22 β-stands and turns, however, Cry1AbⅢ was comprised of 13 α-helices, 21 β-stands and turns. Cry1Ab Ⅰ is the same as Cry1AbⅢ in domain Ⅰ and domainⅢ, and the only difference between them is residues 447-449 form β-sheet in Cry1Ab Ⅰ vs loop in Cry1AbⅢ (Fig. 5). Sequence alignment results (Fig. 6) showed that different residues located in 450, 537, 545 and 568, respectively. The 3-D structural difference between Cry1Ab Ⅰ and Cry1AbⅢ, however, resulted only from residue 450 which is Ala in Cry1Ab Ⅰ and Pro in Cry1AbⅢ.

Cry1AbⅢ had the unique activity against mosquito (Diptera) while the other Cry1Ab were only active against Lepidoptera (Table 3). We speculated that Ala450Pro mutant of Cry1Ab Ⅰ might gain the activity against mosquito because the mutant exhibited the same 3-D structure with Cry1AbⅢ.

3.5 Structural Differences between Cry1Ab Ⅰ and Cry1AbⅣ

There are 610 amino acids in the toxic core of Cry1Ab Ⅰ and 609 in Cry1AbⅣ. The additional residue, which was Trp in residue 182 in Cry1Ab Ⅰ and no corresponding residue in Cry1AbⅣ (Fig. 7), resulting in a shorter α6 in Cry1AbⅣ than that in Cry1Ab Ⅰ (Fig. 8).

3.6 Structural Differences between Cry1AbⅢ and Cry1AbⅣ

There are 610 amino acids in the toxic core of Cry1AbⅢ and 609 in Cry1AbⅣ, the toxic core of Cry1AbⅢ was comprised of 13 α-helices, 21 β-stands and turns, however, Cry1AbⅣ consisted of 13 α-helices, 22 β-stands and turns. Results of 3-D structure comparison revealed the absence of residue Trp in α6 and the additional of β9 (I446-R448) component in Cry1AbⅣ (Fig. 9). The amino acid sequence is different in 182, 450, 537, 545 and 568 according to sequence alignment of Cry1AbⅢ and Cry1AbⅣ (Fig. 10). Furthermore, the differences of residues 182 and 450 result in 3-D structural difference between them.

Table 1. Comparison among three domain structural components of Cry1Ab toxin

		Cry1Ab Ⅰ	Cry1Ab Ⅱ	Cry1AbⅢ	Cry1AbⅣ
Domain Ⅰ	α1	P35-S48	P35-E49	P35-S48	P35-S48
	α2	A54-W65	A54-G66	A54-W65	A54-W65
	α3	P70-I84	P70-I84	P70-I84	P70-I84
	α4	E90-A119	E90-A119	E90-A119	E90-A119
	α5	P124-A149	P 124-A149	P 124-A149	P 124-A149
	α6	Q154-W182	Y153-W182	Q154-W182	Q154-R181
	α7	A186-V218	A186-V218	A186-V218	A185-V217
	α8	S223-Y250	S223-Y250	S223-Y250	S222-Y249
	β1	I267-T269	I267-T269	I267-T269	I266-T268
Domain Ⅱ	α9	P271-N275	P271-N275	P271-N275	P270-N274
	α10	S283-S290	S283-S290	S283-S290	S282-S289
	β2	I299-H310	I299-H310	I299-H310	I298-H309
	β3	E313-S324	E313-S324	E313-S324	E312-S323
	β4	Y359-R368	Y359-R368	Y359-R368	Y358-R367
	β5	L380-Y390	L380-L390	L380-Y390	L379-Y389
	β6	A399-Y401	---	A399-Y401	A398-Y400
	β7	T406-D408	---	T406-D408	T405-D407
	α11	S409-E412	S410-E413	S409-E412	S408-E411
	α12	P422-G425	P423-G426	P422-G425	P421-G424
	β8	H428-V433	---	H428-V433	H427-V432
	β9	I447-R449	V449-R451	---	I446-R448
	β10	F453-H457	S456-W458	F453-H457	F452-H456
	β11	N464-I466	D467-I469	N464-I466	N463-I465
	β12	T472-P475	T475-P478	T472-P475	T471-P474
	α13	---	L479-K481	---	---
Domain Ⅲ	β13	T480-L482	---	T480-L482	T479-L481
	β14	S487-V489	S489-V491	S487-V489	S486-V488
	β15	I499-R502	I501-E504	I499-R502	I498-R501
	β16	G506-I515	I509-I516	G506-I515	G505-I514
	β17	Y523-S531	Y524-S532	Y523-S531	Y522-S530
	β18	L535-I541	L536-I542	L535-I541	L534-I540
	β19	R544-F551	R545-F552	R544-F551	R543-F550
	α14	S563-S565	S564-S566	S563-S565	S562-S564
	β20	R567-G570	R568-G571	R567-G570	R566-G569
	β21	S581-H589	S582-H590	S581-H589	S580-H588
	β22	V597-P606	V598-P607	V597-P606	V596-P605

---lack of component,
The components highlighted in red color represent the main differences between Cry1Ab Ⅰ and other types proteins;
those in green represent the main differences between Cry1Ab Ⅱ and other types proteins; and those in blue represent
the main differences between Cry1AbⅣ and other types proteins

3.7 Structural Differences between Cry1Ab Ⅱ and the other three Groups

There are significant differences among Cry1Ab Ⅱ and other groups from secondary structure and 3-D structure comparison (Fig. 11). A few of the components α1, α2, α6 and some loops differ in their locations in domain Ⅰ. The other differences among them in domain Ⅰ is in Cry1Ab Ⅱ, the absence of β6, β7and β8 and the presence of additional α13 components in comparison with Cry1Ab Ⅰ and Cry1AbⅣ, whereas the absence of β6, β7and β9 and the presence of additional α13 components

in comparison with Cry1AbⅢ, and a few of the components α11, α12, β9, β10, β11 and β12 differ in their locations in domain Ⅱ. Compared to other groups, Cry1Ab Ⅱ have different locations of almost all components and the absence of β13 in domainⅢ. The amino acid sequence alignment can explain why Cry1Ab Ⅱ have so striking differences, number of different points where they locate in residue 207, 382, 383, 386-400, 402, 403, 405, 406, 407, 411, 431, 433, 434, 439, 449, 454-456, 459-461, 466-468, 482-489, 495 and 504-508 between Cry1Ab Ⅰ and Cry1Ab Ⅱ, 207, 382, 383, 386-400, 402, 403, 405, 406, 407, 411, 431, 433, 434, 439, 449, 452,

454, 455, 456, 459, 460, 461, 466, 467, 468, 482-489, 495, 504-508, 540, 548 and 571 between Cry1AbⅡand Cry1AbⅢ, 182, 207, 382, 383, 386-400, 402, 403, 405-407, 431, 433, 434, 439, 449, 454-456, 459-461, 466-468, 482-489, 495 and 504-508 between Cry1AbⅡand Cry1AbⅣ, respectively (Fig. 12).

a

b

c

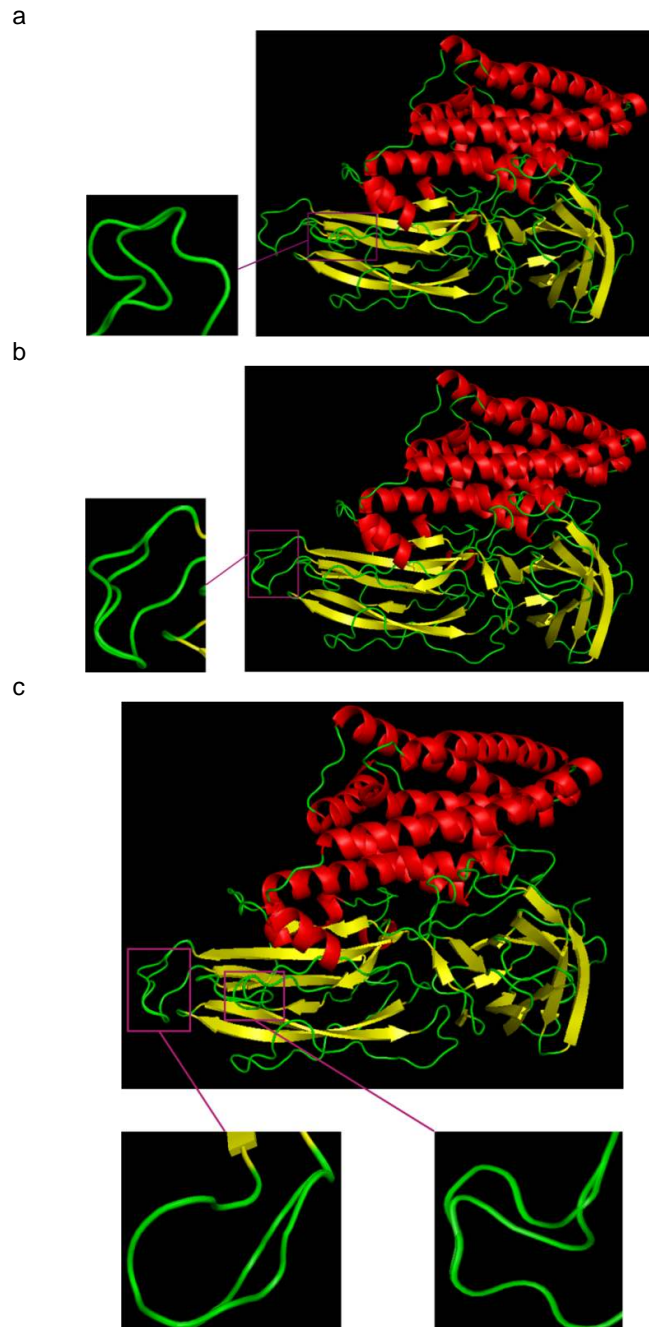**Fig. 4. Structural comparison among the subgroups of Cry1AbI**
The residues highlighted in red color represent helix; those in yellow represent stand and turn; and those in green represent coli and are generated using Pymol software. a the 3-D structural comparison between Cry1Ab1 and Cry1Ab31. b the 3-D structural comparison between Cry1Ab1 and Cry1Ab33. c the 3-D structural comparison between Cry1Ab31 and Cry1Ab33
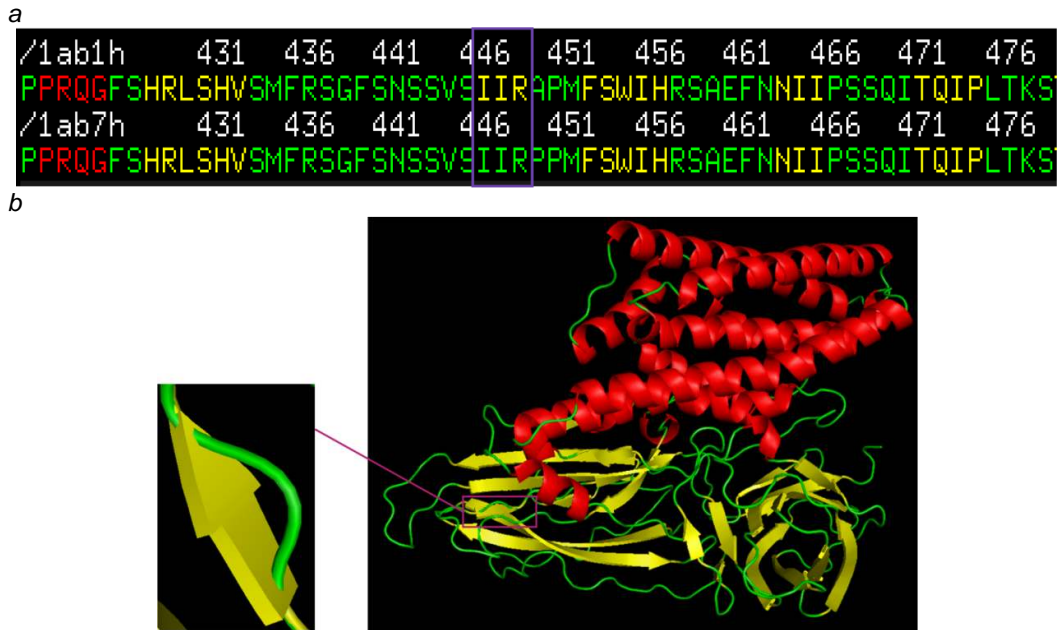
a

b

Fig. 5. Structural comparison between Cry1AbI and Cry1AbIII
The residues highighted in red color represent helix;those in yellow represent stand and turn;and those in green represent coli and are generated using Pymol software. a the secondary structural comparison between Cry1AbI and Cry1AbIII. b the 3-D structural comparison between Cry1AbI and Cry1AbIII. The difference between them is Cry1AbIII lack of one β-sheets in domainII.

```
          . . . . . . . 430. . . . . . 440. . . . . . . 450. . . . . . 460. . . . . . 470. . . . . . 480
Cry1Ab I    PPRQGFSHRLSHVSMFRSGFSNSSVSIIRAPMFSWIHRSAEFNNIIPSSQITQIPLTKST
Cry1Ab III  PPRQGFSHRLSHVSMFRSGFSNSSVSIIRPPMFSWIHRSAEFNNIIPSSQITQIPLTKST
            ****************************.****************************

          . . . . . . . 490. . . . . . 500. . . . . . 510. . . . . . 520. . . . . . 530. . . . . . 540
Cry1Ab I    NLGSGTSVVKGPGFTGGDILRRTSPGQISTLRVNITAPLSQRYRVRIRYASTTNLQFHTS
Cry1Ab III  NLGSGTSVVKGPGFTGGDILRRTSPGQISTLRVNITAPLSQRYRVRIRYASTTNLQLHTS
            ********************************************************.***

          . . . . . . . 550. . . . . . 560. . . . . . 570. . . . . . 580. . . . . . 590. . . . . . 600
Cry1Ab I    IDGRPINQGNFSATMSSGSNLQSGSFRTVGFTTPFNFSNGSSVFTLSAHVFNSGNEVYID
Cry1Ab III  IDGRIINQGNFSATMSSGSNLQSGSFRIVGFTTPFNFSNGSSVFTLSAHVFNSGNEVYID
            ****.*********************** ****************************
```

Fig. 6. The amino acid sequence alignment of Cry1AbI and Cry1AbIII
The first line represent Cry1AbI and second line represent Cry1AbIII. The different residues located in 450, 537, 545 and 568, respectively

```
          . . . . . . . 190. . . . . . 200. . . . . . 210. . . . . . 220. . . . . . 230. . . . . . 240
Cry1Ab I    RWGFDAATINSRYNDLTRLIGNYTDHAVRWYNTGLERVWGPDSRDWIRYNQFRRELTLTV
Cry1Ab VI   R-GFDAATINSRYNDLTRLIGNYTDHAVRWYNTGLERVWGPDSRDWIRYNQFRRELTLTV
            * *********************************************************
```

Fig. 7. The amino acid sequence alignment of Cry1AbI and Cry1AbIV
The first line represent Cry1AbI and second line represent Cry1AbIV. There is Trp in residue 182 of Cry1AbI and no corresponding amino acid residue in Cry1AbIV
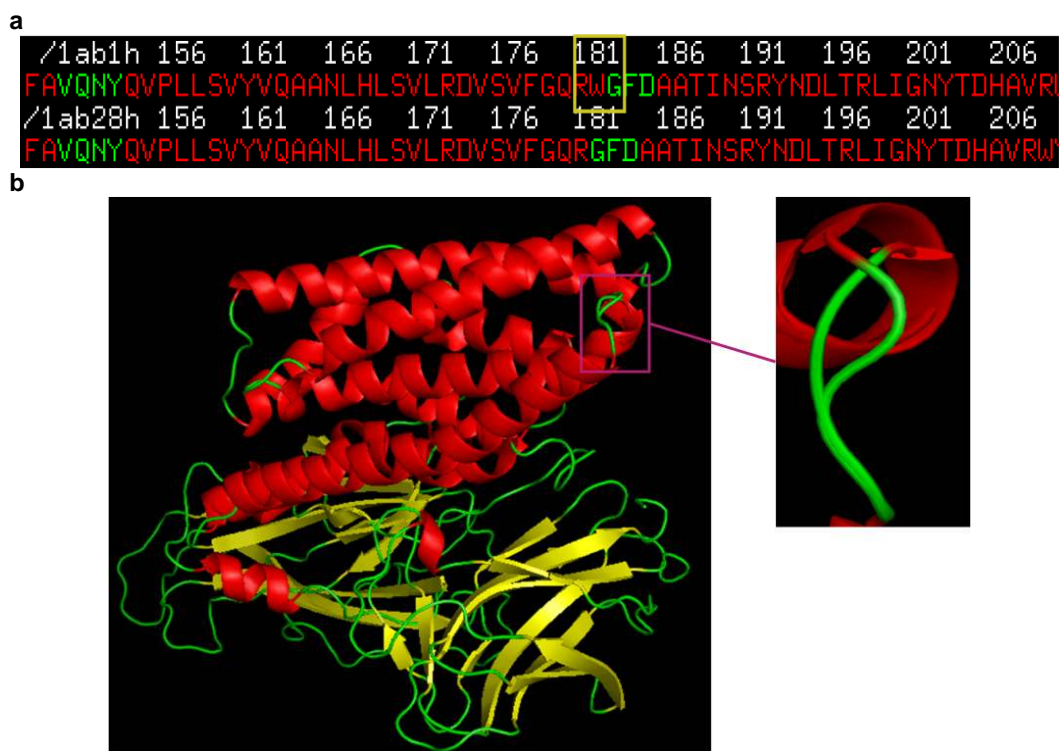
a

```
/1ab1h   156   161   166   171   176   181   186   191   196   201   206
FAVQNYQVPLLSVYVQAANLHLSVLRDVSVFGQRWGFDAATINSRYNDLTRLIGNYTDHAVRW
/1ab28h  156   161   166   171   176   181   186   191   196   201   206
FAVQNYQVPLLSVYVQAANLHLSVLRDVSVFGQRGFDAATINSRYNDLTRLIGNYTDHAVRW
```

b

Fig. 8. Structural comparison between Cry1AbI and Cry1AbIV

The residues highlighted in red color represent helix; those in yellow represent stand and turn; and those in green represent coli and are generated using Pymol software. a the secondary structural comparison between Cry1AbI and Cry1AbIV. b the 3-D structural comparison between Cry1AbI and Cry1AbIV. the different is a shorter α6 in Cry1AbIV than in Cry1AbI

Table 2. A new nomenclature of Cry1Ab proteins based on structure differences of core toxins

Group	Subgroup	Members
Cry1Ab I	Cry1Ab I 1	Cry1Ab1, Cry1Ab3, Cry1Ab4, Cry1Ab5, Cry1Ab6, Cry1Ab8, Cry1Ab9, Cry1Ab10, Cry1Ab11, Cry1Ab12, Cry1Ab13, Cry1Ab14, Cry1Ab15, Cry1Ab16, Cry1Ab17, Cry1Ab18, Cry1Ab19, Cry1Ab20, Cry1Ab21, Cry1Ab22, Cry1Ab23, Cry1Ab24, Cry1Ab25, Cry1Ab26, Cry1Ab27, Cry1Ab29, Cry1Ab30, Cry1Ab31, Cry1Ab32, Cry1Ab33, Cry1Ab34
	Cry1Ab I 2	Cry1Ab31
	Cry1Ab I 3	Cry1Ab33
Cry1Ab II		Cry1Ab2
Cry1Ab III		Cry1Ab7
Cry1Ab IV		Cry1Ab28

There are many differences especially in domain II between Cry1Ab II and the other Cry1Ab groups, however, the available activity data showed that Cry1Ab II had no special activities (Table 3). Either these differences in Cry1Ab II have no obvious influence on insecticidal activities, or much more assays against various insect targets should be performed in details.

Table 3. The reported insecticidal activities of the four groups of Cry1Ab proteins

	Cry1Ab I**	Cry1Ab Ⅱ	Cry1AbⅢ	Cry1AbⅣ
Noctuidae	*Helicoverpa punctigera* *Heliothis virescens* *Mamestra brassicae*	*trichoplusia ni* *heliothis virescens*	ND*	ND*
Lymantridae	*Lymantria dispar* *Orgyia leucostigma*	*Lymantria dispar*	ND*	ND*
Sphingidae	*Manduca sexta*	*Manduca sexta*	ND*	ND*
Pyralidae	*Ostrania nubilalis*	ND*	ND*	ND*
Pieridae	*Pieris brassicae*	ND*	*Pieris brassicae*	ND*
Plutellidae	*plutella xylostella*	ND*	ND*	ND*
Tortricidae	*Choristoneura fumiferana* *Choristoneura occidentalis* *Choristoneura pinus*	ND*	ND*	ND*
Chrysopidae	*Chrysoperla carnea*	ND*	ND*	ND*
Lasiocampidae	*Malacosoma disstria*	ND*	ND*	ND*
Culicidae (Diptera)	ND*	ND*	*Aedes aegypti*	ND*

*ND, not determined, **The insecticidal activity data of Cry1Ab Ⅰ2 and Cry1Ab Ⅰ3 were not available.

a

b
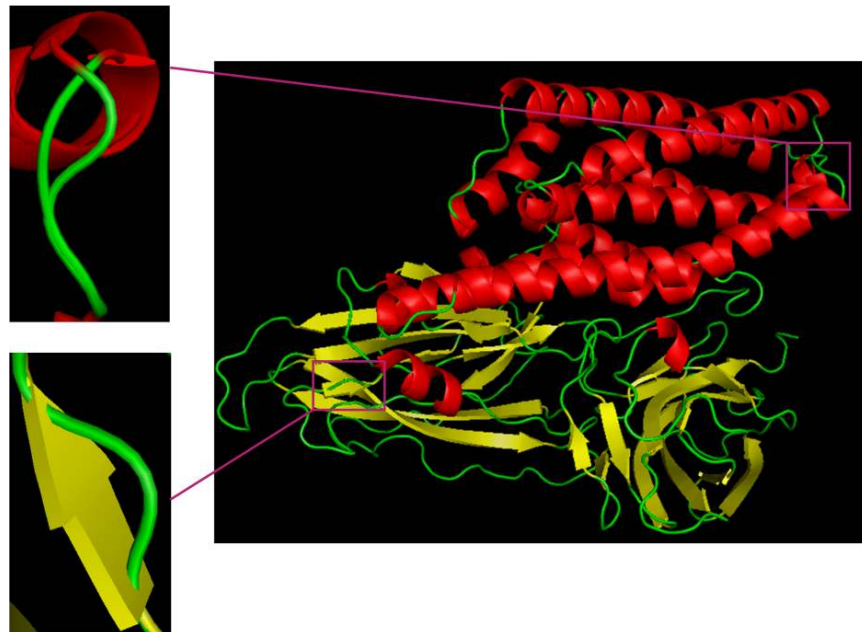
Fig. 9. Structural comparison between Cry1AbⅢ and Cry1AbⅣ
The residues highlighted in red color represent helix; those in yellow represent stand and turn; and those in green represent coli and are generated using Pymol software. a the secondary structural comparison between Cry1AbⅢ and Cry1AbⅣ. b the 3-D structural comparison between Cry1AbⅢ and Cry1AbⅣ. the differences are absence of residue Trp in α6 and the additional of β9 (I446-R448) component in Cry1AbⅣ

```
          . . . . . . 190. . . . . . 200. . . . . . 210. . . . . . 220. . . . . . 230. . . . . . 240
Cry1Ab III   RWGFDAATINSRYNDLTRLIGNYTDHAVRWYNTGLERVWGPDSRDWIRYNQFRRELTLTV
Cry1Ab VI    R-GFDAATINSRYNDLTRLIGNYTDHAVRWYNTGLERVWGPDSRDWIRYNQFRRELTLTV
             *  *********************************************************

          . . . . . . 430. . . . . . 440. . . . . . 450. . . . . . 460. . . . . . 470. . . . . . 480
Cry1Ab III   PPRQGFSHRLSHVSMFRSGFSNSSVSIIRPPMFSWIHRSAEFNNIIPSSQITQIPLTKST
Cry1Ab VI    PPRQGFSHRLSHVSMFRSGFSNSSVSIIRAPMFSWIHRSAEFNNIIPSSQITQIPLTKST
             ***********************************,***************************

          . . . . . . 490. . . . . . 500. . . . . . 510. . . . . . 520. . . . . . 530. . . . . . 540
Cry1Ab III   NLGSGTSVVKGPGFTGGDILRRTSPGQISTLRVNITAPLSQRYRVRIRYASTTNLQLHTS
Cry1Ab VI    NLGSGTSVVKGPGFTGGDILRRTSPGQISTLRVNITAPLSQRYRVRIRYASTTNLQFHTS
             *******************************************************:.***

          . . . . . . 550. . . . . . 560. . . . . . 570. . . . . . 580. . . . . . 590. . . . . . 600
Cry1Ab III   IDGRIINQGNFSATMSSGSNLQSGSFRIVGFTTPFNFSNGSSVFTLSAHVFNSGNEVYID
Cry1Ab VI    IDGRPINQGNFSATMSSGSNLQSGSFRTVGFTTPFNFSNGSSVFTLSAHVFNSGNEVYID
             ****.*******************.**********************************
```

Fig. 10. The amino acid sequence alignment of Cry1AbIII and Cry1AbIV
The first line represent Cry1AbIII and second line represent Cry1AbIV. The amino acid sequence is different in 182, 450, 537, 545 and 568

a

b
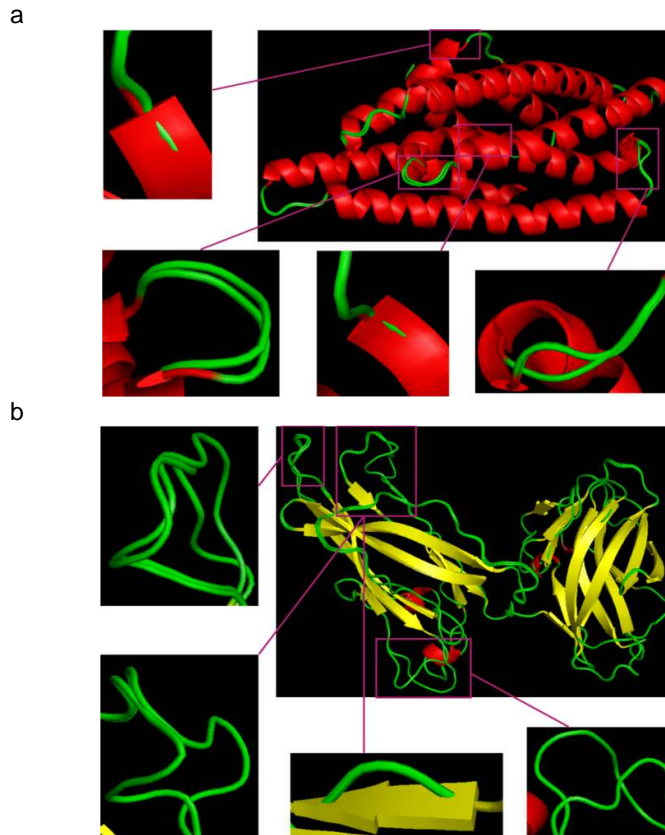
Fig. 11. Structural comparison among Cry1AbI, Cry1AbIII, Cry1AbIV and Cry1AbII
The residues highlighted in red color represent helix; those in yellow represent stand and turn; and those in green represent coli and are generated using Pymol software. a the 3-D structural comparison of domain I among Cry1AbI, Cry1AbIII, Cry1AbIV and Cry1AbII. A few of the components α1, α2, α6 and some loops differ in their locations in domain I. the other differences among them in domain I is in Cry1AbII, the absence of β6, β7and β8 and presence of additional α13 components in comparison with Cry1AbI and Cry1AbIV. b the 3-D structural comparison of domain II and domain III among Cry1AbI, Cry1AbIII, Cry1AbIVand Cry1AbII. the Cry1AbII absence of β6, β7and β9 and presence of additional α13 components in comparison with Cry1AbIII and a few of the components α11, α12, β9, β10, β11 and β12 differ in their locations in domain II. And Cry1AbII have different locations of almost all components and the absence of β13 in domain III

a

```
. . . . . . . 190. . . . . . 200. . . . . . 210. . . . . . 220. . . . . . 230. . . . . . 240
```
Cry1Ab I   `RWGFDAATINSRYNDLTRLIGNYTDHAVRWYNTGLERVWGPDSRDWIRYNQFRRELTLTV`
Cry1Ab II `RWGFDAATINSRYNDLTRLIGNYTDHRVRWYNTGLERVWGPDSRDWIRYNQFRRELTLTV`
```
*************************** ********************************
```
```
. . . . . . . 370. . . . . . 380. . . . . . 390. . . . . . 400. . . . . . 410. . . . . . 420
```
Cry1Ab I   `TLSSTLYRRPFNIGINNQQLSVLDGTEFAYGTSSNLPSAVY-RKSGTVDSLDEIPPQNNN`
Cry1Ab II `TLSSTLYRRPFNIGINNQQLSGPDGGRICLWNLLKFGQPPYTEKAEPVDSPDEIPPQNNN`
```
******************** **  :.  .  ::  .  *  *:  *** *********
```
```
. . . . . . . 430. . . . . . 440. . . . . . 450. . . . . . 460. . . . . . 470. . . . . . 480
```
Cry1Ab I   `VPPRQGFSHR-LSHVSMFRSGFSNSSVSIIRAPM-FSWIHRSAEFNNIIPSSQITQIPLT`
Cry1Ab II `VPPRQGFSHRCLAYVSMFYSGFSNSSVSVIRAPNDSSWTYCSAEFGDVIPSSQITQIPLT`
```
********** *:.:**** *********.**** ** : ****.::***********
```
```
. . . . . . . 490. . . . . . 500. . . . . . 510. . . . . . 520. . . . . . 530. . . . . . 540
```
Cry1Ab I   `KSTNLGSGTSVVKGPGFTGGDILRRTSPGQISTLRVNITAPLSQRYRVRIRYASTTNLQF`
Cry1Ab II `KLQSW-LWNSVVKGLGFTGGDILEELT-GQISTLRVNITAPLSQRYRVRIRYASTTNLQF`
```
* .     ***** ********   :  *****************************
```

b

```
. . . . . . . 190. . . . . . 200. . . . . . 210. . . . . . 220. . . . . . 230. . . . . . 240
```
Cry1Ab II   `RWGFDAATINSRYNDLTRLIGNYTDHRVRWYNTGLERVWGPDSRDWIRYNQFRRELTLTV`
Cry1Ab III `RWGFDAATINSRYNDLTRLIGNYTDHAVRWYNTGLERVWGPDSRDWIRYNQFRRELTLTV`
```
*************************** ********************************
```
```
. . . . . . . 370. . . . . . 380. . . . . . 390. . . . . . 400. . . . . . 410. . . . . . 420
```
Cry1Ab II   `TLSSTLYRRPFNIGINNQQLSGPDGGRICLWNLLKFGQPPYTEKAEPVDSPDEIPPQNNN`
Cry1Ab III `TLSSTLYRRPFNIGINNQQLSVLDGTEFAYGTSSNLPSAVY-RKSGTVDSLDEIPPQNNN`
```
******************** **  :.  .  ::  .  *  *:  *** *********
```
```
. . . . . . . 430. . . . . . 440. . . . . . 450. . . . . . 460. . . . . . 470. . . . . . 480
```
Cry1Ab II   `VPPRQGFSHRCLAYVSMFYSGFSNSSVSVIRAPNDSSWTYCSAEFGDVIPSSQITQIPLT`
Cry1Ab III `VPPRQGFSHR-LSHVSMFRSGFSNSSVSIIRPPM-FSWIHRSAEFNNIIPSSQITQIPLT`
```
********** *:.:**** *********.**.* ** : ****.::***********
```
```
. . . . . . . 490. . . . . . 500. . . . . . 510. . . . . . 520. . . . . . 530. . . . . . 540
```
Cry1Ab II   `KLQSW-LWNSVVKGLGFTGGDILEELT-GQISTLRVNITAPLSQRYRVRIRYASTTNLQF`
Cry1Ab III `KSTNLGSGTSVVKGPGFTGGDILRRTSPGQISTLRVNITAPLSQRYRVRIRYASTTNLQL`
```
* .     ***** ********   :  ***************************:
```
```
. . . . . . . 550. . . . . . 560. . . . . . 570. . . . . . 580. . . . . . 590. . . . . . 600
```
Cry1Ab II   `HTSIDGRPINQGNFSATMSSGSNLQSGSFRTVGFTTPFNFSNGSSVFTLSAHVFNSGNEV`
Cry1Ab III `HTSIDGRIINQGNFSATMSSGSNLQSGSFRIVGFTTPFNFSNGSSVFTLSAHVFNSGNEV`
```
******* ******************************** ********************
```

c

```
. . . . . . . 190. . . . . . 200. . . . . . 210. . . . . . 220. . . . . . 230. . . . . . 240
```
Cry1Ab II `RWGFDAATINSRYNDLTRLIGNYTDHRVRWYNTGLERVWGPDSRDWIRYNQFRRELTLTV`
Cry1Ab VI `R-GFDAATINSRYNDLTRLIGNYTDHAVRWYNTGLERVWGPDSRDWIRYNQFRRELTLTV`
```
* ************************* ********************************
```
```
. . . . . . . 370. . . . . . 380. . . . . . 390. . . . . . 400. . . . . . 410. . . . . . 420
```
Cry1Ab II `TLSSTLYRRPFNIGINNQQLSGPDGGRICLWNLLKFGQPPYTEKAEPVDSPDEIPPQNNN`
Cry1Ab VI `TLSSTLYRRPFNIGINNQQLSVLDGTEFAYGTSSNLPSAVY-RKSGTVDSLDEIPPQNNN`
```
******************** **  :.  .  ::  ..  *  *:  *** *********
```
```
. . . . . . . 430. . . . . . 440. . . . . . 450. . . . . . 460. . . . . . 470. . . . . . 480
```
Cry1Ab II `VPPRQGFSHRCLAYVSMFYSGFSNSSVSVIRAPNDSSWTYCSAEFGDVIPSSQITQIPLT`
Cry1Ab VI `VPPRQGFSHR-LSHVSMFRSGFSNSSVSIIRAPM-FSWIHRSAEFNNIIPSSQITQIPLT`
```
********** *:.:**** *********:**** ** : ****.::***********
```
```
. . . . . . . 490. . . . . . 500. . . . . . 510. . . . . . 520. . . . . . 530. . . . . . 540
```
Cry1Ab II `KLQSW-LWNSVVKGLGFTGGDILEELT-GQISTLRVNITAPLSQRYRVRIRYASTTNLQF`
Cry1Ab VI `KSTNLGSGTSVVKGPGFTGGDILRRTSPGQISTLRVNITAPLSQRYRVRIRYASTTNLQF`
```
* .     ***** ********   :  *****************************
```

Fig. 12. The amino acid sequence alignment of Cry1AbI, Cry1AbIII, Cry1AbIV and Cry1AbII

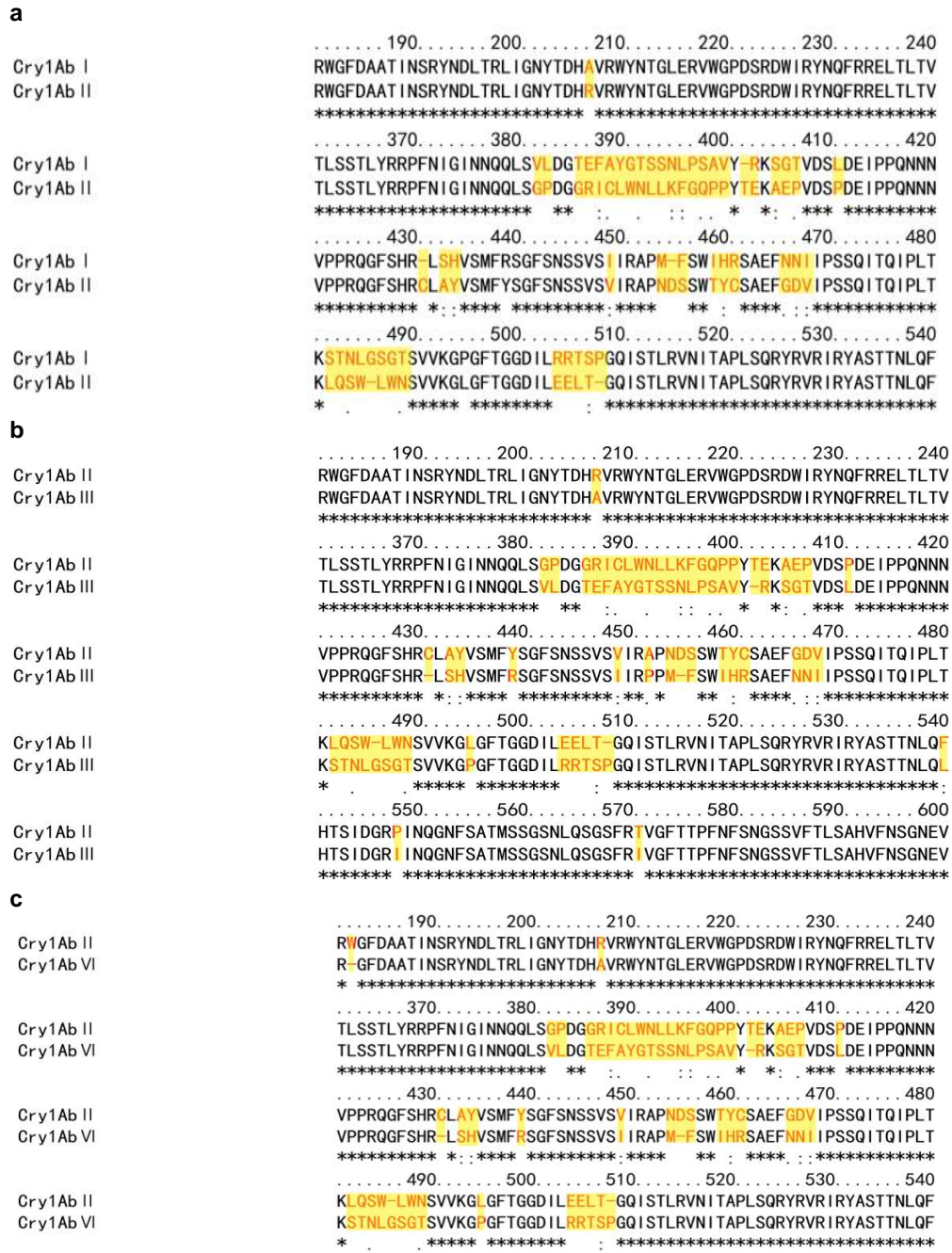*a The amino acid sequence alignment of Cry1AbI and Cry1AbII. the first line represent Cry1AbI and second line represent Cry1AbII. the number of different points where they locate in residue 207, 382, 383, 386-400, 402, 403, 405, 406, 407, 411, 431, 433, 434, 439, 449, 454-456, 459-461, 466-468, 482-489, 495 and 504-508. b The amino acid sequence alignment of Cry1AbII and Cry1AbIII. the first line represent Cry1AbII and second line represent Cry1AbIII. the number of different points where they locate in residue 207, 382, 383, 386-400, 402, 403, 405, 406, 407, 411, 431, 433, 434, 439, 449, 452, 454, 455, 456, 459, 460, 461, 466, 467, 468, 482-489, 495, 504-508, 540, 548 and 571. c The amino acid sequence alignment of Cry1AbII and Cry1AbIV. the first line represent Cry1AbII and second line represent Cry1AbIV. the number of different points where they locate in residue 182, 207, 382, 383, 386-400, 402, 403, 405-407, 431, 433, 434, 439, 449, 454-456, 459-461, 466-468, 482-489, 495 and 504-508*

4. DISCUSSION

As showed in this study, all 34 available Cry1Ab proteins, which were listed in the old nomenclature on the basis of their full-length amino acid sequences sharing at least 95% homologies, can be divided into four groups and subgroups based on toxic core structural differences. This change from a sequence-based to a structure-based nomenclature allows closely related proteins to be ranked together and provide researchers function information.

Domain Ⅰ of four Cry1Ab groups are similar (Table 1), which have 8 α-helices and is thought to be directly involved in membrane penetration and pore formation after binding to the specific receptor on surface of midgut [28]. In the pore formation model of Cry toxin action, binding to cadherin facilitates the proteolytic removal of domain Ⅰ α-1 promoting oligomer formation [29]. Nuria et al. showed the helix α-3 (the same to α-4 in this study) in domain Ⅰ that could form coiled-coli structures important for oligomerization [30]. In other reports the mutations Arg-93 and Ala-92 (located at the beginning of α-3) of Cry1Ab severely affected toxicity and correlated with loss of pore formation [31,32], and substitutions in residue Arg-99 also resulted in a complete loss of pore activity [33]. In addition, characterization of domain Ⅰ α-4 (the same to α-5 in this study) mutants revealed that in contrast to α-3 mutants described above, the point mutations in α-4 were able to form oligomeric structures [34]. Li et al. [8] suggested that the helical hairpin α4-α5 (the same to α5-α6 in this study) act as the initiator of the membrane related allosteric mechanism of penetration commonly known as umbrella model, and Thanate et al. [35] signified that the polarity at the α4-α5 loop residue Asn-166 was directly involved in ion permeation. All data revealed that domain Ⅰ was an essential component for pore-formation so that the structure of four groups Cry1Ab of domain Ⅰ was conservative and exactly alike. It is possible that mutation aimed to an increase in these helices will improve the pore forming activity of Cry1Ab toxin.

The main differences among the four Cry1Ab groups in domain Ⅱ are the length and location of one of the two loops joining the apical β-stands. Loop α9-α10 represent loop α8 in other papers and the other three receptor binding loops called loops 1, 2 and 3, respectively. In this study, loop α8, loop 1 (β2-β3) and loop 2 (β4-β5)

are similar whereas loop 3 is different among the four groups. Loop 3 of Cry1Ab Ⅰ and Cry1AbⅣ is loop β8-β9 (residues: S^{434}MFRSGFSNSSVS^{446}), loop α12-β9 (residues: F^{427}SHRCLAYVSMFYSGFSNSSVS^{448}) in Cry1Ab Ⅱ and loop β8-β10 (residues: S^{434}MFRSGFSNSSVSIIRPPM^{452}) in Cry1Ab Ⅲ, respectively. Loops 2 and α8 of Cry1Ab are reported to have a binding affinity for *M. sexta* Bt receptor (BtR) [36], and loops 2 and 3 are reported to have a binding affinity for *H. virescens* BtR [37]. In addition, the mutations G439A and F440A significantly reduced toxicity toward *M. sexta* and *H. virescens* and in contrast, mutants S438A, S441A, N442A, and S443A were similar or only marginally less toxic to the insects compared to the wild-type toxin [38]. Both of Cry1Ab Ⅰ and Cry1Ab Ⅱ have activity against *M. sexta* and *H. virescens* (Table 2), so the difference of loop 3 between Cry1Ab Ⅰ and Cry1Ab Ⅱ has no influence on activity. No data reveal Cry1Ab Ⅲ and Cry1Ab Ⅳ have activity against *M. sexta* and *H. virescens*, but the structure of Cry1AbⅣ is similar with Cry1Ab Ⅰ, so it is possible that Cry1Ab Ⅳ have activity against *M. sexta* and *H. virescens.*

Domain Ⅲ, which consists of 2 β-sheets in a jellyroll conformation, has been implicated in determining specificity, then Cry1Ab Ⅱ have different structure of domainⅢ compare to other three groups. Swapping domain Ⅲ between toxins, such as Cry1Ab become more active against *Spodoptera exigua* when its domainⅢ was replaced by part of that of Cry1Ca [39], this result shows domain Ⅲ have influence on insecticidal activity. In addition, mutations in domainⅢ of Cry1Aa had an effect on both ion channel activity and membrane permeability [40]. DomainⅢ could play a role in protecting the toxin against further cleavage by gut proteases [41].

5. CONCLUSION

Based on the template of Cry1Aa, we have built 3-D structure models for all the current 34 Cry1Ab proteins. Based on the secondary structure pattern, four different groups were identified and named as Cry1Ab Ⅰ, Cry1Ab Ⅱ, Cry1AbⅢ, and Cry1Ab Ⅳ. The three Cry1Ab proteins, Cry1Ab2, Cry1Ab7 and Cry1Ab28 were recognized as Cry1AbⅡ, Cry1AbⅢ, and Cry1Ab Ⅳ, respectively. The other 31 Cry1Ab proteins were grouped as Cry1Ab Ⅰ, and were further

divided into three subgroups based on 3-D structural differences. The structural differences among different Cry1Ab groups and subgroups were analyzed in details. The insecticidal activities of different Cry1Ab groups and subgroups were also discussed. It was worthy to speculate that the only difference in 3-D structure, residues 447-449 form β-sheet in Cry1AbⅠ vs loop in Cry1AbⅢ, resulted in Cry1AbⅠ inactive vs Cry1AbⅢ active against mosquito. The results provided new insights into structure-function relationship of Cry1Ab proteins.

ACKNOWLEDGEMENTS

COMPETING INTERESTS

Authors have declared that no competing interests exist.

REFERENCES

1. Swamy HM, Asokan R, Mahmood R. In silico structural 3D modelling of novel Cry1Ib9 and Cry3A toxins from local isolates of *Bacillus thuringiensis*. Indian J Microbiol. 2014;54(1):94-103.
2. Hofmann C, Vanderbruggen H, Hofte H, Van Rie J, Jansens S, Van Mellaert H. Specificity of *Bacillus thuringiensis* delta-endotoxins is correlated with the presence of high-affinity binding sites in the brush border membrane of target insect midguts. Proc Natl Acad Sci USA. 1988; 85(21):7844-8.
3. Knowles BH, Ellar DJ. Colloid-osmotic lysis is a general feature of the mechanism of action of *Bacillus thuringiensis* δ-endotoxins with different insect specificity. Biochimica et Biophysica Acta (BBA)-General Subjects. 1987;924(3):509-18.
4. Gazit E, La Rocca P, Sansom MS, Shai Y. The structure and organization within the membrane of the helices composing the pore-forming domain of *Bacillus thuringiensis* delta-endotoxin are consistent with an "umbrella-like" structure of the pore. Proc Natl Acad Sci USA. 1998;95(21):12289-94.
5. Crickmore N, Zeigler D, Feitelson J, Schnepf E, Van Rie J, Lereclus D, et al. Revision of the nomenclature for the *Bacillus thuringiensis* pesticidal crystal proteins. Microbiol Mol Biol R. 1998;62(3): 807-13.
6. Grochulski P, Masson L, Borisova S, Pusztai-Carey M, Schwartz JL, Brousseau R, et al. *Bacillus thuringiensis* CryIA(a) insecticidal toxin: Crystal structure and channel formation. J Mol Biol. 1995;254(3): 447-64.
7. Morse R, Yamamoto T, Stroud R. Structure of Cry2Aa suggests an unexpected receptor binding epitope. Structure. 2001;9(5):409-17.
8. Li JD, Carroll J, Ellar DJ. Crystal structure of insecticidal delta-endotoxin from *Bacillus thuringiensis* at 2.5 A resolution. Nature. 1991;353(6347):815-21.
9. Galitsky N, Cody V, Wojtczak A, Ghosh D, Luft JR, Pangborn W, et al. Structure of the insecticidal bacterial delta-endotoxin Cry3Bb1 of *Bacillus thuringiensis*. Acta Crystallogr D Biol Crystallogr. 2001;57(8): 1101-9.
10. Boonserm P, Mo M, Angsuthanasombat C, Lescar J. Structure of the functional form of the mosquito larvicidal Cry4Aa toxin from *Bacillus thuringiensis* at a 2.8-angstrom resolution. J Bacteriol. 2006;188(9):3391-401.
11. Boonserm P, Davis P, Ellar DJ, Li J. Crystal structure of the mosquito-larvicidal toxin Cry4Ba and its biological implications. J Mol Biol. 2005;348(2):363-82.
12. Guo S, Ye S, Liu Y, Wei L, Xue J, Wu H, et al. Crystal structure of *Bacillus thuringiensis* Cry8Ea1: An insecticidal toxin toxic to underground pests, the larvae of *Holotrichia parallela*. J Struct Biol. 2009;168(2):259-66.
13. Hui F, Scheib U, Hu Y, Sommer RJ, Aroian RV, Ghosh P. Structure and glycolipid binding properties of the nematicidal protein Cry5B. Biochemistry. 2012;51(49): 9911-21.
14. Gutierrez P, Alzate O, Orduz S. A theoretical model of the tridimensional structure of *Bacillus thuringiensis* subsp. medellin Cry 11Bb toxin deduced by homology modelling. Mem Inst Oswaldo Cruz. 2001;96(3):357-64.
15. Zhao XM, Xia LQ, Ding XZ, Wang FX. The theoretical three-dimensional structure of *Bacillus thuringiensis* Cry5Aa and its biological implications. Protein J. 2009; 28(2):104-10.

16. Xia LQ, Zhao XM, Ding XZ, Wang FX, Sun YJ. The theoretical 3D structure of *Bacillus thuringiensis* Cry5Ba. J Mol Model. 2008; 14(9):843-8.

17. Dehury B, Sahu M, Sahu J, Sarma K, Sen P, Modi MK, et al. Structural analysis and molecular dynamics simulations of novel delta-endotoxin Cry1Id from *Bacillus thuringiensis* to pave the way for development of novel fusion proteins against insect pests of crops. J Mol Model. 2003;19(12):5301-16.

18. Zhao XM, Zhou PD, Xia LQ. Homology modeling of mosquitocidal Cry30Ca2 of *Bacillus thuringiensis* and its molecular docking with N-acetylgalactosamine. Biomed Environ Sci. 2012;25(5):590-6.

19. Mahalakshmi A, Shenbagarathai R. Homology modeling of Cry10Aa toxin from *B. thuringiensis* israelensis and *B. thuringiensis* subsp. LDC-9. J Biomol Struct Dyn. 2010;28(3):363-78.

20. Kashyap S, Singh B, Amla D. Homology modelling deduced 3-D structure of *Bacillus thuringiensis* Cry1Ab17 toxin. ScienceAsia. 2010;36(4):280-5.

21. Kashyap S, Singh B, Amla D. Prediction of three-dimensional structure of Cry1Ab21 toxin from *Bacillus thuringiensis* Bt IS5056. J Plant Biochem Biot. 2011;20(1):142-7.

22. Kashyap S, Singh BD, Amla DV. Computational tridimensional protein modeling of Cry1Ab19 toxin from *Bacillus thuringiensis* BtX-2. J Microbiol Biotechnol. 2012;22(6):788-92.

23. Kashyap S. Computational modeling deduced three dimensional structure of Cry1Ab16 toxin from *Bacillus thuringiensis* AC11. Indian J Microbiol. 2012;52(2):263-9.

24. Kashyap S. In silico modeling and functional interpretations of Cry1Ab15 toxin from *Bacillus thuringiensis* BtB-Hm-16. Biomed Res Int. 2013;2013:471636.

25. Biasini M, Bienert S, Waterhouse A, Arnold K, Studer G, Schmidt T, et al. SWISS-MODEL: Modelling protein tertiary and quaternary structure using evolutionary information. Nucleic Acids Res. 2014; 42(Web Server issue):252-8.

26. Pieper U, Eswar N, Davis FP, Braberg H, Madhusudhan MS, Rossi A, et al. MODBASE: A database of annotated comparative protein structure models and associated resources. Nucleic Acids Res. 2006;34(Suppl 1):291-5.

27. Chothia C, Lesk AM. The relation between the divergence of sequence and structure in proteins. The EMBO Journal. 1986;5(4):823-6.

28. Rausell C, Pardo-López L, Sánchez J, Muñoz-Garay C, Morera C, Soberón M, et al. Unfolding events in the water-soluble monomeric Cry1Ab toxin during transition to oligomeric pre-pore and membrane-inserted pore channel. J Biol Chem. 2004;279(53):55168-75.

29. Soberon M, Pardo-Lopez L, Lopez I, Gomez I, Tabashnik BE, Bravo A. Engineering modified Bt toxins to counter insect resistance. Science. 2007; 318(5856):1640-2.

30. Jimenez-Juarez N, Munoz-Garay C, Gomez I, Saab-Rincon G, Damian-Almazo JY, Gill SS, et al. *Bacillus thuringiensis* Cry1Ab mutants affecting oligomer formation are non-toxic to *Manduca sexta* larvae. J Biol Chem. 2007;282(29):21222-9.

31. Wu D, Aronson AI. Localized mutagenesis defines regions of the *Bacillus thuringiensis* delta-endotoxin involved in toxicity and specificity. J Biol Chem. 1992;167(4):2311-7.

32. Chen XJ, Curtiss A, Alcantara E, Dean DH. Mutations in domain I of *Bacillus thuringiensis* delta-endotoxin CryIAb reduce the irreversible binding of toxin to *Manduca sexta* brush border membrane vesicles. J Biol Chem. 1995;270(11):6412-9.

33. Vachon V, Prefontaine G, Coux F, Rang C, Marceau L, Masson L, et al. Role of helix 3 in pore formation by the *Bacillus thuringiensis* insecticidal toxin Cry1Aa. Biochemistry. 2002;41(19):6178-84.

34. Rodriguez-Almazan C, Zavala LE, Munoz-Garay C, Jimenez-Juarez N, Pacheco S, Masson L, et al. Dominant negative mutants of *Bacillus thuringiensis* Cry1Ab toxin function as anti-toxins: demonstration of the role of oligomerization in toxicity. Plos One. 2009;4(5):e5545.

35. Juntadech T, Kanintronkul Y, Kanchanawarin C, Katzenmeier G, Angsuthanasombat C. Importance of polarity of the alpha4-alpha5 loop residue-Asn(166) in the pore-forming domain of the *Bacillus thuringiensis* Cry4Ba toxin: Implications for ion permeation and pore opening. Biochim Biophys Acta. 2014;1838(1 Pt B):319-27.

36. Gomez I, Dean DH, Bravo A, Soberon M. Molecular basis for *Bacillus thuringiensis* Cry1Ab toxin specificity: Two structural

determinants in the *Manduca sexta* Bt-R1 receptor interact with loops alpha-8 and 2 in domain II of Cy1Ab toxin. Biochemistry. 2003;42(35):10482-9.

37. Xie R, Zhuang M, Ross LS, Gomez I, Oltean DI, Bravo A, et al. Single amino acid mutations in the cadherin receptor from Heliothis virescens affect its toxin binding ability to Cry1A toxins. J Biol Chem. 2005;280(9):8416-25.

38. Rajamohan F, Hussain SR, Cotrill JA, Gould F, Dean DH. Mutations at domain II, loop 3, of *Bacillus thuringiensis* CryIAa and CryIAb delta-endotoxins suggest loop 3 is involved in initial binding to lepidopteran midguts. J Biol Chem. 1996;271(41): 25220-6.

39. de Maagd RA, Weemen-Hendriks M, Stiekema W, Bosch D. *Bacillus thuringiensis* delta-endotoxin Cry1C domain III can function as a specificity determinant for *Spodoptera exigua* in different, but not all, Cry1-Cry1C hybrids. Appl Environ Microbiol. 2000;66(4):1559-63.

40. Schwartz JL, Potvin L, Chen XJ, Brousseau R, Laprade R, Dean DH. Single-site mutations in the conserved alternating-arginine region affect ionic channels formed by CryIAa, a *Bacillus thuringiensis* toxin. Appl Environ Microbiol. 1997;63(10):3978-84.

41. Masson L, Tabashnik BE, Mazza A, Prefontaine G, Potvin L, Brousseau R, et al. Mutagenic analysis of a conserved region of domain III in the Cry1Ac toxin of *Bacillus thuringiensis*. Appl Environ Microbiol. 2002;68(1):194-200.

Peer-review history:
The peer review history for this paper can be accessed here:
http://sciencedomain.org/review-history/12676